

Detecting uniform areas for vicarious calibration using Landsat TM imagery: a study using the Arabian and Saharan deserts

Kent Hilbert¹, Mary Pagnutti², and Robert Ryan³, Lockheed Martin Space Operations – Stennis Programs, Stennis Space Center, Mississippi 39529, USA

Vicki Zanoni⁴, NASA Earth Science Applications Directorate, Stennis Space Center, Mississippi 39529, USA

¹Corresponding author. Tel.: 601-979-3654; fax: 601-979-8247; e-mail: kent.hilbert@jsums.edu

² Tel.: 228-688-2135; Fax: 228-688-7694; e-mail: Mary.Pagnutti@ssc.nasa.gov

³ Tel.: 228-688-1868; Fax: 228-688-7694; e-mail: Robert.Ryan@ssc.nasa.gov

⁴ Tel.: 228-688-2305; Fax: 228-688-7455; e-mail: Vicki.Zanoni@ssc.nasa.gov

Detecting uniform areas for vicarious calibration using Landsat TM imagery: a study using the Arabian and Saharan deserts

Abstract

This paper discusses a method for detecting spatially uniform sites needed for radiometric characterization of remote sensing satellites. Such information is critical for scientific research applications of imagery having moderate to high resolutions (<30 -m ground sampling distance (GSD)). Previously published literature indicated that areas within the African Saharan and Arabian deserts contained extremely uniform sites with respect to spatial characteristics. We developed an algorithm for detecting site uniformity and applied it to orthorectified Landsat Thematic Mapper (TM) imagery over eight uniform regions of interest. The algorithm's results were assessed using both medium-resolution (30-m GSD) Landsat 7 ETM+ and fine-resolution (<5 -m GSD) IKONOS multispectral data collected over sites in Libya and Mali. Fine-resolution imagery over a Libyan site exhibited less than 1 percent nonuniformity. The research shows that Landsat TM products appear highly useful for detecting potential calibration sites for system characterization. In particular, the approach detected spatially uniform regions that frequently occur at multiple scales of observation.

1. Introduction

Numerous remote sensing methods, including change detection, atmospheric correction, and the application of various indices, require radiometrically calibrated data (Dingirard and Slater 1999). Researchers needing to verify the accuracy of multispectral image data do not always have access to details about the acquisition systems' calibration methods; therefore, researchers require an effective, cost-efficient method for performing vicarious radiometric calibration. Vicarious calibration methods are those that use well-characterized ground scenes for in-flight calibration (Slater et al. 1996).

There is a need for identifying vicarious calibration sites at several locations/landscapes and scales of observation. The Advanced Very High Resolution Radiometer (AVHRR), the Meteorological Satellite (METEOSAT), Le Systeme Pour l'Observation de la Terre (SPOT), the Ocean Color and Temperature Sensor (OCTS), and the Polarization and Directionality of Earth Reflectances (POLDER) sensor research teams found natural targets useful for accurately achieving absolute radiometric calibration. Although research teams perform preflight radiometric calibrations in optical laboratories and several sensors contain onboard calibration devices, they still encounter problems. Problems include postlaunch instrument degradation, aging of the optics, and outgassing when the instrument leaves the earth's atmosphere. In fact, the POLDER project team completely avoided developing an onboard calibration system because of problems encountered with obtaining accurate measurements from calibration devices onboard SPOT (Hagolle et al., 1999).

This paper discusses a method that detects uniform calibration sites for conducting long-term radiometric vicarious calibrations of current and future passive systems, including Space Imaging's IKONOS and DigitalGlobe's QuickBird sensors. We validated the proposed method using both Landsat ETM+ and IKONOS image data acquired over African desertic environments. The Landsat ETM+ sensor offers one 15-m resolution panchromatic band, six 30-m resolution bands that collect in the visible, near-Infrared, and mid-Infrared portions of the spectrum, and a 60-m resolution thermal band. IKONOS collects four bands of 4-m resolution multispectral imagery in the visible and near-Infrared portions of the spectrum and includes a 1-m resolution panchromatic band (Lillesand and Kiefer, 2000). This research is driven by the need to reduce the costs associated with conducting vicarious radiometric calibrations, especially when ground team deployment is necessary. The ultimate goal involves detecting uniform sites, worldwide, via automated methods. Once stable uniform sites are identified, researchers may obtain a given multispectral sensor system's imagery of a uniform site acquired over multiple dates to study the acquisition system's temporal stability. Performing such characterizations should optimize and/or reduce ground team deployment requirements, thus reducing the cost of conducting vicarious radiometric calibrations.

2. Background

Scientists use uniform sites for radiometrically calibrating sensors in three different ways: classical reflectance vicarious calibration, radiance calibration methods, and temporal stability studies. Researchers often choose reflectance-based vicarious calibrations for evaluating system radiometry (Dinguirard and Slater, 1999; Kaufman and

Holben, 1993; Meygret et al., 2000; Slater et al., 1987; Slater et al., 1994; Slater et al., 1996; Thome et al., 1993). Applying this approach often involves imaging an extensively large, spatially uniform area of interest. Significant coordination is required for the satellite to image a site when a research institution's ground team is present. The ground team measures atmospheric conditions and surface reflectance properties at or near the time of scene acquisition. Ground measurements are then used in estimating the top-of-the-atmosphere radiance for comparison with the provided sensor radiance values. However, successful data acquisition may be hampered by weather and by changes in satellite tasking priorities. Repeated attempts to synchronize ground team support with satellite data acquisition, along with equipment requirements and logistical problems, may make ground team deployment costly. Increasing the number of viable sites makes this process easier to implement.

Scientists also use alternate methods for evaluating radiometry. One such method involves two or more systems acquiring coincident or near coincident imagery. This alternative is referred to as the radiance-based method (Dingirard and Slater, 1999; Slater et al., 1987; Slater et al., 1994; Slater et al., 1996). This method involves comparing imagery from a highly characterized system, such as the Landsat-7 (L7) Enhanced Thematic Mapper-Plus (ETM+) sensor, to imagery from a system undergoing characterization. ETM+ exhibits excellent radiometry and its bands are similar to those of IKONOS, making it an excellent candidate for use in a radiance-based method (Goddard Space Flight Center, 2000). Locating virtually cloud-free sites and acquiring routine coincident collects with ETM+ or another well-characterized system provides an avenue

for systematically checking a given system's radiometry. Identifying numerous uniform areas optimizes coincident collection opportunities.

The third way in which uniform sites are used in characterizing system radiometry requires temporally stable sites. Temporal stability, typically correlated with low annual precipitation, proves critical for long-term studies. Minimal cloud cover typically distinguishes stable sites and increases the probability of a high-quality acquisition. Desert areas often exhibit such characteristics (Dingirard and Slater, 1999; Kaufman and Holben, 1993; Meygret et al., 2000), and research teams associated with monitoring the temporal calibration drifts of the AVHRR, the Along-Track Scanning Radiometer (ATSR-2), METEOSAT, and SPOT sensors use desert areas that meet these characteristics (Hagolle et al., 1999). Researchers, in fact, developed a procedure for selecting desert areas based upon spatial uniformity criteria using METEOSAT-4 visible data (Cosnefroy et al., 1993). Hagolle et al. (1999), in discussing the use of deserts for the low-frequency multiangular calibration of the POLDER sensor, reported that after the removal of directional effects, the residual root mean square variations, which represent random temporal variability, have relative values of 1-2 percent for desert areas identified as spatially uniform.

The present work introduces an approach different in terms of application and technique. Past researchers used imagery having coarse spatial resolution, e.g., 2.5-km GSD METEOSAT-4 visible imagery, for locating uniform sites. Earth Satellite Corporation's (EarthSat) GeoCoverTM TM products (orthorectified Landsat TM imagery) purchased via the NASA Earth Science Enterprise (ESE) Scientific Data Purchase (SDP) program, which offer global coverage of the terrestrial surface at a 28.5-m GSD, provide

the opportunity for locating uniform sites at relatively high spatial resolution. We took the initiative of developing a systematic method for detecting uniform sites having small scene footprints, similar to those collected by Space Imaging's IKONOS sensor, and applied it to Landsat TM imagery covering several of the sites identified by Cosnefroy et al. (1993). In validating the method, we purchased L7 ETM+ and IKONOS imagery acquired over areas that we identified as uniform using the Landsat TM imagery. We found that small artifacts, including focal plane array (FPA) striping, become visible when Space Imaging's IKONOS sensor collects imagery over uniform sites.

3. Study sites and data

Through the SDP, EarthSat provided orthorectified Landsat TM data covering the African continent. The entire EarthSat SDP product consists of global coverage of orthorectified Landsat Multispectral Scanner (MSS) scenes from the 1970s and Landsat TM scenes spanning the late 1980s to the early 1990s. For both MSS and TM datasets, EarthSat and NASA personnel attempted to select scenes with less than 20 percent cloud cover. Nevertheless, some scenes contain cloud cover exceeding 20 percent but overall global coverage contains less than 20 percent. We validated that the horizontal positional accuracy for the scenes fell within EarthSat's contractual specifications that called for $\pm 100\text{-m}$ and $\pm 50\text{-m}$ Root Mean Square Error (RMSE) for Landsat MSS and Landsat TM scenes, respectively.

From these orthorectified Landsat TM datasets, we selected eight validated image scenes in the African Sahara and Arabian deserts that contained previously identified uniform sites (Cosnefroy, Leroy, and Briottet, 1996). They noted the spatial and temporal

stability of these sites using METEOSAT-4 visible imagery. METEOSAT-4 collected visible imagery at a 2.5-km GSD compared to the IKONOS sensor's 4-m GSD. Landsat TM's 28.5-m GSD, 88 times better than METEOSAT-4 visible imagery's spatial resolution, approaches existing and planned high spatial resolution commercial data sets. Table 1 (extracted from Cosnefroy, Leroy, and Briottet, 1996) provides the location of each site and characterizes the environment, e.g., the annual clear day percentages and the average annual precipitation. Table 2 contains a list of the orthorectified Landsat TM scenes used, and Figure 1 shows the average reflectances derived from the blue, green, red, and near-infrared (NIR) spectral bands for each scene. We derived radiance and reflectance values from published Landsat TM radiometric calibration coefficients and the radiance/reflectance conversion routine (EOSAT, 1986). Figure 1 shows that average band reflectances ranged from 20 percent in the blue band to 58 percent in the NIR band, indicating relatively bright scenes. High reflectance proves essential for simplifying the radiative transfer atmospheric corrections. Figure 2 provides a map showing the locations of the imagery.

4. Methods

We developed a multispectral Figure of Merit (FOM) to quantify spatial nonuniformity, equally weighting the importance of each band. The algorithm, shown in Equation (1), calculates the mean of the root sum squares of the spatial variations of several bands of interest for a defined window. A low FOM calculation indicates high spatial uniformity. The FOM is a measure of band average nonuniformity of the scene.

The window is chosen by considering both the characteristics of the sensor and the problem being addressed. The window is a subimage for which the FOM is calculated.

$$FOM = \frac{1}{\sqrt{N}} \sqrt{\sum_{i=1}^N \left(\frac{s_i}{\bar{X}_i} \right)^2} \quad (1)$$

Where:

s_i = radiance standard deviation of the image or sub-image's spectral band i ,

\bar{X}_i = mean radiance of the image or sub-image's spectral band i , and

N = number of spectral bands analyzed

First, we computed the FOM for an entire given Landsat TM scene (in radiance) using IKONOS-like bands 1 through 4. Table 3 shows the similarities between the first four multispectral bands of Landsat TM and IKONOS. IKONOS' NIR band, slightly different from Landsat TM, minimizes atmospheric water absorption. The calculation provides a means of evaluating a given Landsat TM scene's overall uniformity. The coefficient of variation (COV), $\frac{s_i}{\bar{X}_i}$ in Equation (1), removes the influence of the data's magnitude, allowing direct comparison of relative variability.

We also attempted to detect uniform sites for IKONOS-specific validation. Using a moving window of user-specified dimensions, we calculated and geographically located the area within a Landsat TM scene having the lowest FOM for the specified window size. For this research effort, we used a window having the dimensions of 10972.5 m x 997.5 m (385 by 35 pixels at a 28.5-m GSD). We define these dimensions as ~11 km x 1 km throughout the rest of the paper. We selected this window size because it covers the nominal 11-km IKONOS swath and provides a sufficient number of in-track pixels for statistically estimating the mean and standard deviation at the Landsat TM spatial resolution. We ignored adjacency effects for scenes discussed in this paper because the adjacent areas exhibit similar reflectance values. Figure 3 provides a conceptual illustration of the calculation. We stepped the window of interest in one-pixel intervals (28.5-m GSD) within the scene, and calculated the window FOM for each interval. The user-defined window is centered at the current pixel and the FOM is computed using all pixels contained within the window. We discarded invalid FOM values that result when the window surrounding a given pixel does not contain a complete set of pixels, e.g., along the boundaries of the image. Future improvements may include using image mosaics. We focused on specific row/paths because of radiometric and seasonal differences associated with mosaicking.

5. Results

Table 4 summarizes our initial analysis that estimated the nonuniformity of the entire 185-km x 185-km areas contained in each of the eight selected Landsat TM scenes.

In this case, the 'Mali 1' site, path 198/row 47 collected by Landsat TM 5 on January 7, 1986, exhibited the lowest average FOM (6.5 percent nonuniformity).

Table 5 and Figure 4 provide the results of our analysis related to detecting specific ~11-km x 1-km uniform areas for IKONOS-specific vicarious calibration. Research results indicated that an ~11-km x 1-km area in Libya, centered on 23° 54' 10.25" N, 13° 17' 06.36" E, exhibited the greatest uniformity, i.e., the lowest FOM (0.0086). This means that the area detected is 0.86 percent nonuniform. Figure 5 shows the location of this block (outlined in yellow) within the Landsat TM scene (path 187/row 43 collected by Landsat 5 on January 13, 1987). Visual analysis indicated that the automated algorithm detected an area relatively devoid of sand dunes. Figure 6 shows a spectral profile transect of the area identified. Within the 11-km x 1-km window, the scene shows few spatial frequency variations. Appendix A provides an image gallery that shows the locations of the ~11-km x 1-km areas, also highlighted in yellow, exhibiting the lowest FOM's in the remaining seven Landsat TM scenes.

6. Validation of Results

We validated the FOM technique by comparing Landsat TM, IKONOS, and L7 ETM+ imagery. We acquired, through the SDP program, two Standard Original (georectified) IKONOS images over Mali and Libya. Space Imaging processed these images with Modulation Transfer Function Compensation (MTFC). MTFC, an edge sharpening technique, improves object recognition. Unpublished internal studies indicate that the effects of MTFC are negligible over uniform scenes. An IKONOS scene acquired over a slightly different region of Mali provided a means for comparing not only the

temporal, but also the spatial stability of a location within one of the analyzed Landsat TM scenes. An IKONOS scene over Libya, centered on the coordinates of the lowest FOM ~11-km x 1-km area (0.86 percent nonuniformity) detected using Landsat TM imagery, provided a means for evaluating the algorithm for a chosen moving window size.

We also purchased two L7 ETM+ datasets that covered the above-mentioned areas in Mali and Libya. This offered an opportunity for using the radiance-based approach and examining temporal changes.

The chosen validation technique involved subsetting the imagery both spectrally and spatially. We used only the blue, green, red, and near-infrared spectral bands common to Landsat TM, L7 ETM+, and IKONOS. First, we spatially subset the Landsat TM and L7 ETM+ images to a given IKONOS scene's geographical extent. Then we converted the Landsat TM, IKONOS, and L7 ETM+ images from digital numbers to radiance values. The next two subsections discuss the findings of the validation exercise.

6.1 Case 1: Mali

We acquired an IKONOS scene collected on November 3, 2000, over an area in Mali centered on 19° 09' 25.48" N, 4° 53' 24.34" W. A Landsat TM image previously obtained through the SDP (path 198, row 47, collected on January 1, 1986) contained the region imaged by the IKONOS sensor. We also purchased L7 ETM+ imagery collected on March 13, 2001 and having the same path and row as the Landsat TM imagery.

Prior to comparing overall spatial uniformity, a visual comparison illustrated the temporal stability of the region imaged. Figure 7 shows that the spatial features remained fairly unchanged over a period of 16 years.

We then compared the spatial nonuniformity of each scene by calculating the COV for each band and an overall FOM for each image. Figure 8 compares the resulting COV and FOM calculations. The IKONOS image typically exhibited higher COV values than the Landsat TM and L7 ETM+ images. This result is to be expected since Landsat TM's 28.5-m and L7 ETM+'s 30-m GSD smoothes out small-scale variation. For this site, IKONOS' band COVs and overall FOM are less than 4 percent, indicating that the site is extremely uniform. These results illustrate the usefulness of EarthSat's orthorectified Landsat TM imagery for detecting uniform areas for calibrating the IKONOS sensor.

6.2 Case 2: Libya

Of the eight EarthSat SDP orthorectified Landsat TM scenes analyzed using the FOM algorithm, a scene (Landsat 5, path 187 row 42, acquired on January 13, 1987) covering a region in Libya contained an ~11-km x 1-km area that exhibited the lowest FOM (0.86 percent nonuniformity). We acquired, through the SDP program, an IKONOS Standard Original image covering this area. The IKONOS image, acquired on April 4, 2001, and centered on 23° 56' 23.71" N, 13° 14' 36.71" E, is shown in Figure 9. The stretch applied to this image resulted in the appearance of IKONOS' three focal planes. Generally, when a sensor system's focal planes are not optimally calibrated, the focal planes become visible when the sensor images uniform areas.

Figure 10 shows the array differences between the focal planes via a cross-sectional plot of spectral bands normalized to the spectral means. The ability to detect artifacts, including focal planes, indicates that the scene exhibits sufficient uniformity to measure relative radiometry. NOTE: Space Imaging has since corrected the focal plane problem.

We also purchased L7 ETM+ imagery collected on May 19, 2001 and having the same path and row as the EarthSat product. Figure 11 shows 11-km x 11-km Landsat TM, L7 ETM+, and IKONOS imagery covering the ~11-km x 1-km area of interest (yellow bounding boxes), and it shows a comparison of these images in terms of COV and FOM. We speculate that the large, dark feature in the southwest portion of the IKONOS image is a playa lake. The IKONOS ~11- km x 1-km subset exhibits a slightly lower FOM value. The COV also appears lower in IKONOS' blue and green spectral bands. We theorize that this occurred because the blue and green Landsat TM bands' COV approached their signal-to-noise ratio (SNR) limits. Eventually, the COV becomes the inverse of SNR for a perfectly uniform scene. Figure 11's graph shows that IKONOS band COVs and overall FOM for this site are less than 1 percent, indicating extreme uniformity for this site. These results further illustrate the FOM algorithm's potential for detecting uniform sites for vicarious sensor calibration using Landsat TM imagery.

7. Summary and Conclusions

This paper introduces a practical method for detecting uniform sites for vicarious calibration that potentially decreases the need for fielded ground teams. The method involves applying a Figure of Merit algorithm that quantifies a site's nonuniformity using a window of a user-specified dimension with bands of equal weight. Using Landsat TM data, we detected eight ~11-km x 1-km sites in the African Saharan and Arabian deserts having less than 3 percent nonuniformity. The detected sites exhibit high reflectance values, which assist in measuring the top-of-the-atmosphere radiance. One ~11-km x 1-km site within

Libya exhibited less than 1 percent nonuniformity. COV and FOM comparisons between Landsat TM, L7 ETM+, and IKONOS imagery over regions within both Mali and Libya validate the proposed FOM algorithm's usefulness. The banding observed in the IKONOS scene over an area of Libya further validates the FOM algorithm's usefulness for detecting uniform areas.

Future activities include detecting optimal calibration sites for Earth Observing One (EO-1), Advanced Spaceborne Thermal Emission and Reflection Radiometer (ASTER), and other systems. Such an activity could also address the effect of varying the window size on FOM and COV calculations because sensor specifications, in terms of nominal scene size, often differ. Acquiring more L7 ETM+ imagery over these sites potentially allows temporal change analysis. Examining the role of adjacency effects would also prove beneficial. Long-term plans include exploring the utility of coincident collects for radiance verification and cross comparisons. Work continues on developing generalized software for searching the entire SDP Landsat TM image archive to detect uniform sites of various dimensions. This long-term effort shall provide the first systematic high-spatial resolution survey of the entire Earth surface. In the short-term, we are focusing on the desert Southwest of the United States. Future research could involve optimizing the weighting for specific bands of interest for specific applications.

Acknowledgements

We wish to thank the many NASA Earth Science and Applications Directorate (ESAD) and Lockheed Martin Remote Sensing Directorate team members for their assistance in making this research project a success. Employees of DATASTAR (a

subcontractor that provides Information Technology support to Lockheed Martin's Remote Sensing Directorate) ensured the accessibility of archived SDP orthorectified Landsat TM data and of the recently acquired IKONOS imagery. We also thank the many NASA ESAD and Lockheed Martin Remote Sensing Directorate team members that provided input in an internal peer-review. And last, but definitely not least, we thank the Lockheed Martin Remote Sensing Directorate's technical writers for grammatical editing and formatting.

References

- Cosnefroy, H., Briottet, X. and Leroy, M., 1993. Characterization of desert areas with METEOSAT-4 data for the calibration of optical satellite sensors. SPIE, International Symposium on Optical Engineering and Photonics, vol. 1938, Orlando, April 1993.
- Cosnefroy, H., Leroy, M. and Briottet, X., 1996. Selection and characterization of Saharan and Arabian desert sites for the calibration of optical satellite sensors. *Remote Sensing of Environment*, 58: 101-114.
- Dingirard, M. and Slater, P. N., 1999. Calibration of space-multispectral imaging sensors: a review. *Remote Sensing of Environment*, 68: 194-205.
- EOSAT, 1986. Landsat Technical Notes, August 1986.
- Goddard Space Flight Center, 2000. Landsat 7 enhanced Thematic Mapper-Plus (7) data quality and geographic coverage. URL: http://landsat.gsfc.nasa.gov/announcements/data_qual_feb2000.html. Accessed 05/30/01.

- Hagolle, O., Goloub, P., Deschamps, P., Cosnefroy, H., Briottet, X., Bailleul, T., Nicolas, J., Parol, F., Lafrance, B. and Herman, M., 1999. Results of POLDER in-flight calibration. *IEEE Transactions of Geoscience and Remote Sensing*, 37 (3): 1550-1566.
- Kaufman, Y. J. and Holben, B. N., 1993. Calibration of the AVHRR visible and near-IR bands by atmospheric scattering, ocean glint and desert reflection. *International Journal of Remote Sensing*, 14: 21-52.
- Lillesand, T. and Kiefer, R., 2000. *Remote Sensing and Image Interpretation*, 4th Edition, John Wiley & Sons, Inc., New York.
- Meygret, A., Briottet, X., Henry, P. and Hagolle, O., 2000. Calibration of SPOT4 HRVIR and VEGETATION cameras over the Rayleigh scattering. *Proc. SPIE 4135*, pp. 302-313.
- Schowengerdt, R., 1997. *Remote Sensing: Models and Methods for Image Processing*, 2nd Edition, Academic Press, New York.
- Slater, P. N., Biggar, S. F., Holm, R. G., Jackson, R. D., Mao, Y., Moran, M. S., Palmer, J. M. and Yuan, B., 1987. Reflectance- and radiance-based methods for the in-flight absolute calibration of multispectral sensors. *Remote Sensing of Environment*, 22: 11-37.
- Slater, P. N., Biggar, S. F., Thome, K. J., Gellman, D. I. and Spyak, P. R., 1994. The in-flight radiometric calibration of ASTER by reference to well-characterized scenes. *Proc. SPIE 2317*, pp. 49-60.

- Slater, P. N., Biggar, S. F., Thome, K. J., Gellman, D. I. and Spyak, P. R., 1996. Vicarious radiometric calibration of EOS sensors. *Journal of Atmospheric and Oceanic Technology*, 13: 349-359.
- Thome, K. J., Gellman, D. I., Parada, R. J., Biggar, S. F., Slater, P. N. and Moran, M. S., 1993. In-flight radiometric calibration of Landsat-5 Thematic Mapper from 1984 to present. *Proc. SPIE* 1938, pp. 126-130.

Table 1. Location and climatic characteristics of the selected study areas.

Site	Latitude (deg)	Longitude (deg)	Annual % of Clear Days	Avg. Monthly Precipitation (mm)
Egypt 1	27° 07' 12" N	26° 06' 00" E	65	0.4
Libya 1	28° 33' 00" N	23° 23' 24" E	59	0.8
Libya 4	24° 25' 12" N	13° 21' 00" E	55	1.4
Algeria 3	30° 19' 12" N	07° 39' 36" E	48	2.8
Algeria 4	30° 02' 24" N	05° 35' 24" E	50	2.2
Algeria 2	26° 05' 24" N	01° 22' 48" W	49	2.2
Mali 1	19° 07' 12" N	04° 51' 00" W	27	4.1
Mauritania 1	19° 24' 00" N	09° 18' 00" W	25	4.8

Table 2. EarthSat GeoCoverTM TM imagery used in the analysis.

Associated Site (Cosnefroy et al. 1996)	Landsat TM Path / Row	Acquisition Date	Landsat TM Platform #	Scene Center Geographic Coordinates (Latitude and Longitude)
Egypt 1	179 / 041	10/20/87	5	27° 25' 12.8017" N, 26° 36' 56.4497" E
Libya 4	181 / 040	01/19/87	5	28° 51' 34.9092" N, 23° 53' 22.6894" E
Libya 1	187 / 043	01/13/87	5	24° 32' 35.8606" N, 13° 31' 16.5639" E
Algeria 3	192 / 039	01/27/88	4	30° 17' 26.2917" N, 07° 15' 37.7491" E
Algeria 4	193 / 039	01/07/87	5	30° 17' 21.5617" N, 05° 41' 36.5624" E
Algeria 2	197 / 042	02/04/87	5	25° 59' 05.0692" N, 01° 32' 51.6537" W
Mali 1	198 / 047	01/07/86	5	18° 46' 50.0472" N, 04° 53' 28.2929" W
Mauritania 1	201 / 047	01/26/88	4	18° 46' 37.0622" N, 09° 28' 16.8981" W

Table 3. Landsat TM and IKONOS Multispectral Band Comparison (1st four bands).

Landsat TM	Ikonos
0.450 – 0.520 μm (Blue)	0.445 – 0.516 μm (Blue)
0.520 – 0.600 μm (Green)	0.506 – 0.595 μm (Green)
0.630 – 0.690 μm (Red)	0.632 – 0.698 μm (Red)
0.760 – 0.900 μm (NIR)	0.757 – 0.853 μm (NIR)

Table 4. African site nonuniformity at full Landsat TM scene size.

Associated Site (Cosnefroy et al. 1996)	Landsat TM Path / Row	Average FOM (%)
Egypt 1	179 / 041	6.7
Libya 4	181 / 040	8.1
Libya 1	187 / 043	9.9
Algeria 3	192 / 039	13.6
Algeria 4	193 / 039	12.7
Algeria 2	197 / 042	10.6
Mali 1	198 / 047	6.5
Mauritania 1	201 / 047	10.5

Table 5. Locations of ~11-km x 1-km sites exhibiting the lowest FOMs.

Associated Site (Cosnefroy et al. 1996)	Center Geographic Coordinates of 11 km x 1 km Areas Exhibiting Lowest FOM's (Latitude and Longitude)
Egypt 1	27° 15' 26.51" N, 27° 16' 47.09" E
Libya 4	29° 25' 58.14" N, 23° 51' 16.30" E
Libya 1	23° 54' 10.25" N, 13° 17' 06.36" E
Algeria 3	29° 34' 55.27" N, 06° 32' 58.51" E
Algeria 4	30° 49' 32.29" N, 05° 56' 56.83" E
Algeria 2	25° 11' 15.81" N, 00° 52' 22.84" W
Mali 1	19° 23' 29.41" N, 04° 01' 37.66" W
Mauritania 1	19° 31' 23.59" N, 09° 31' 00.34" W

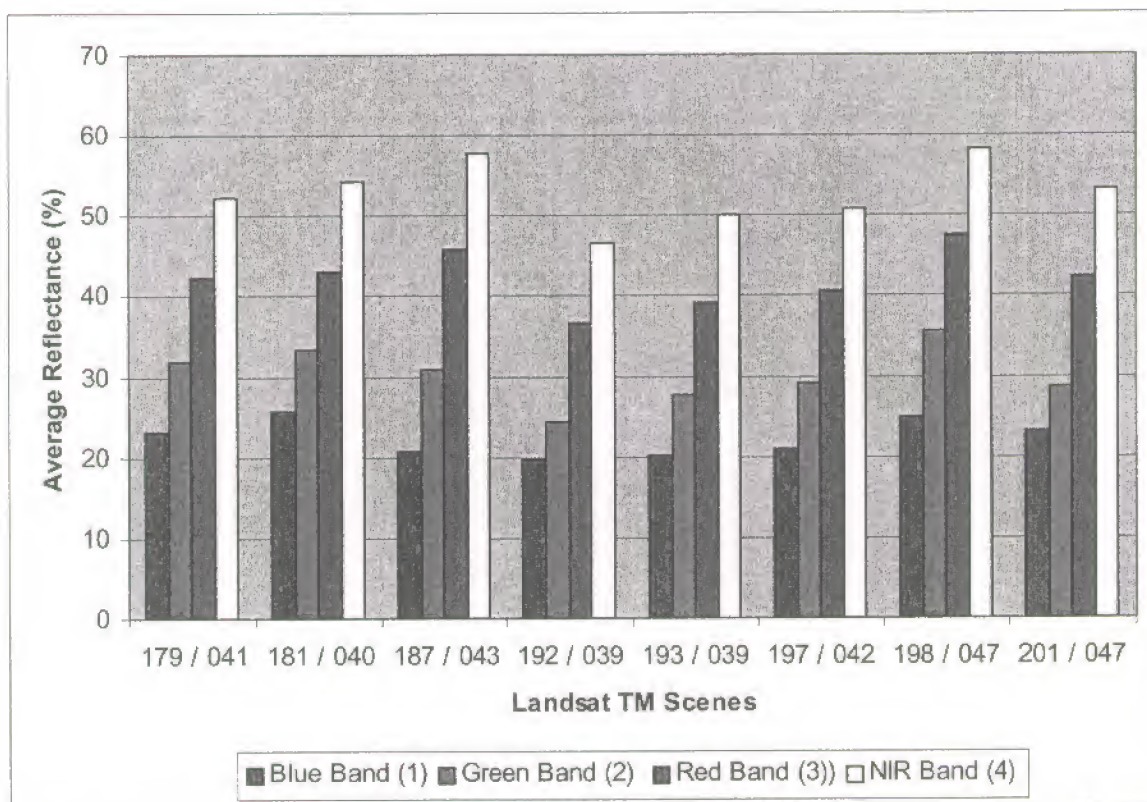


Figure 1. Average reflectance values of orthorectified Landsat TM scenes analyzed.

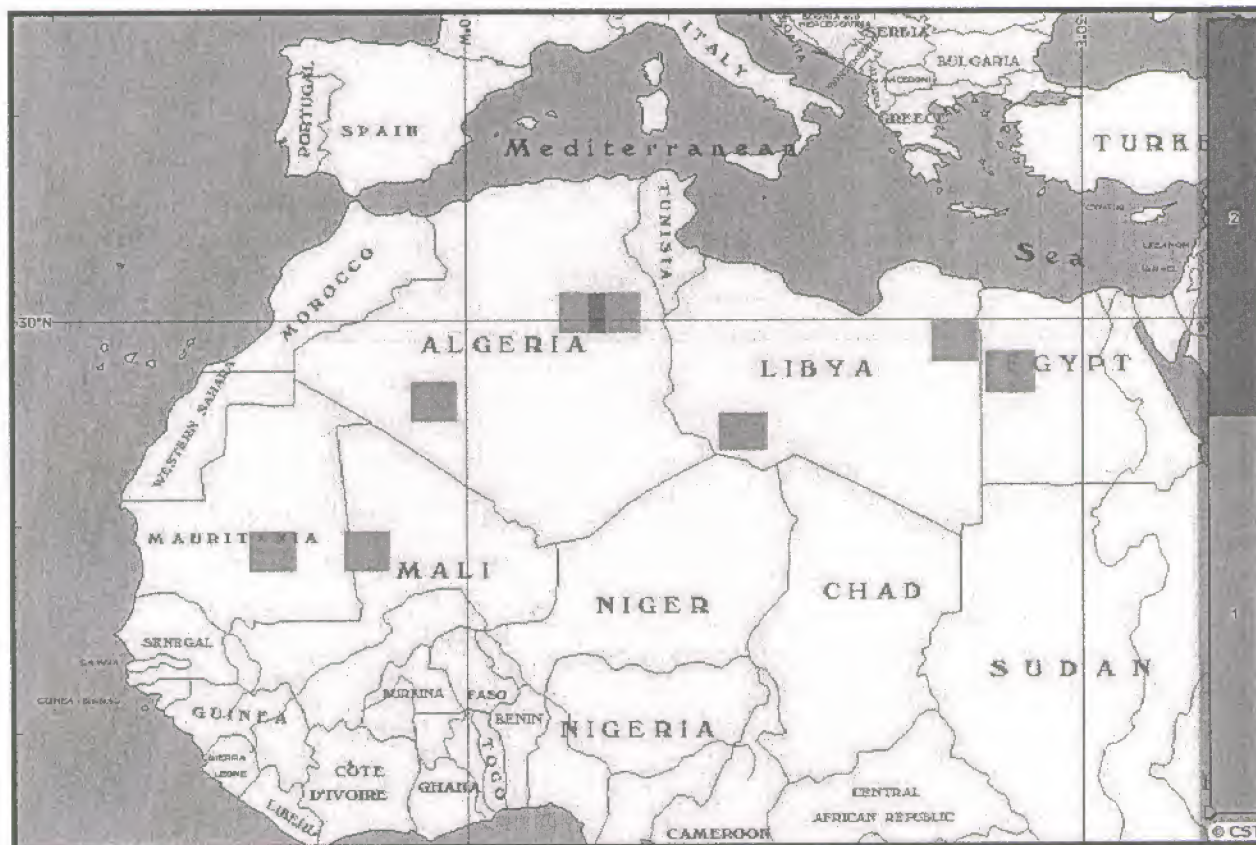


Figure 2. African site Landsat TM Path/Row coverage. The green rectangles show the spatial extent of each Landsat TM scene while the red area represents overlapping scenes.

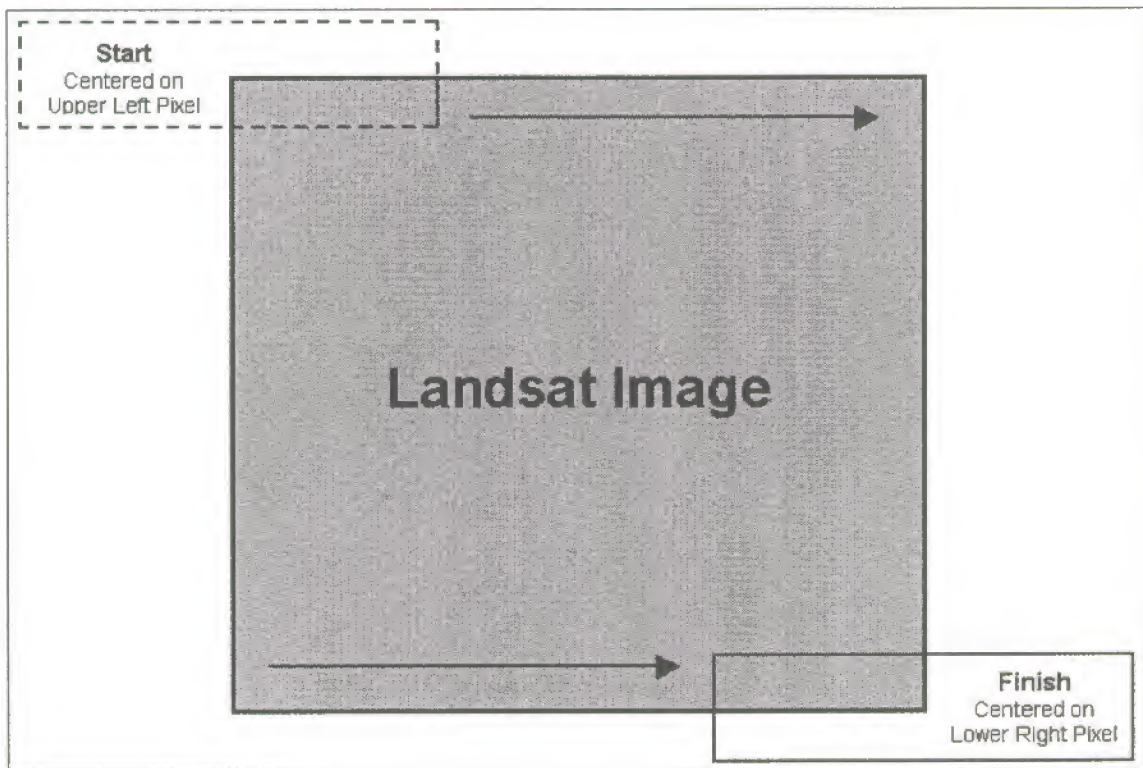


Figure 3. A graphic illustration of the moving window concept.

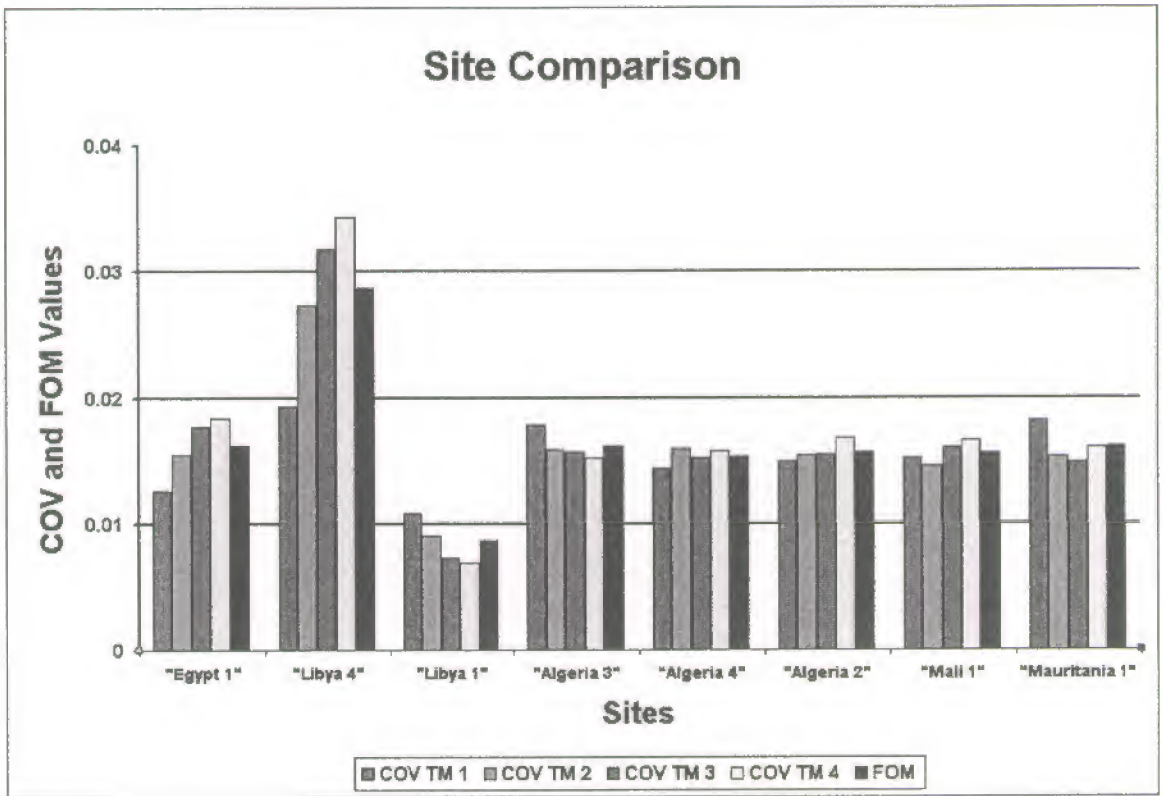


Figure 4. A chart comparing the ~11-km x 1-km areas found to have the lowest FOMs.

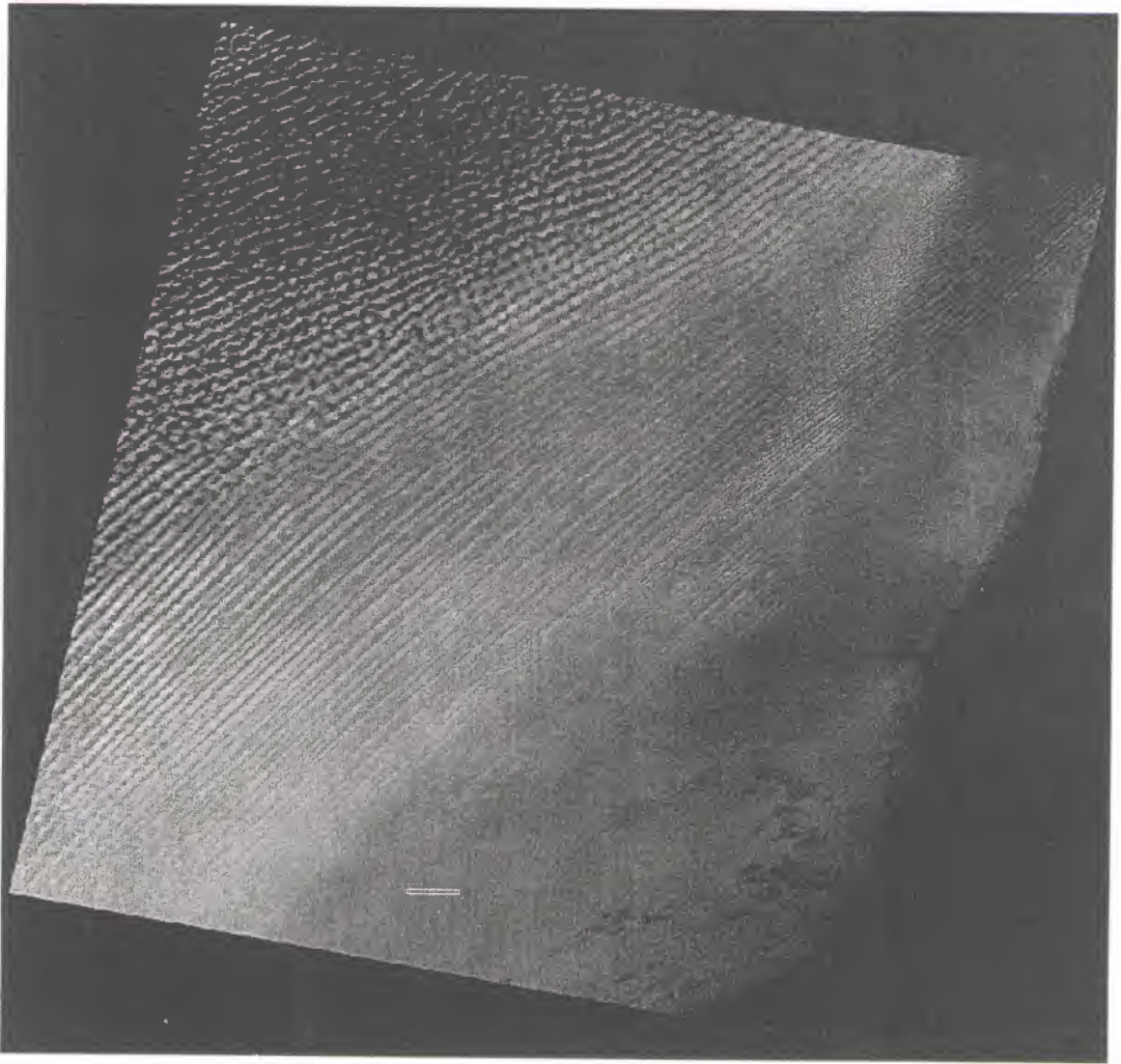


Figure 5. The orthorectified Landsat TM image (p187r42_5t870113) containing the most uniform
~ 11- km x 1-km area 'Libya 1' (yellow rectangle). RGB: 3, 2, 1.

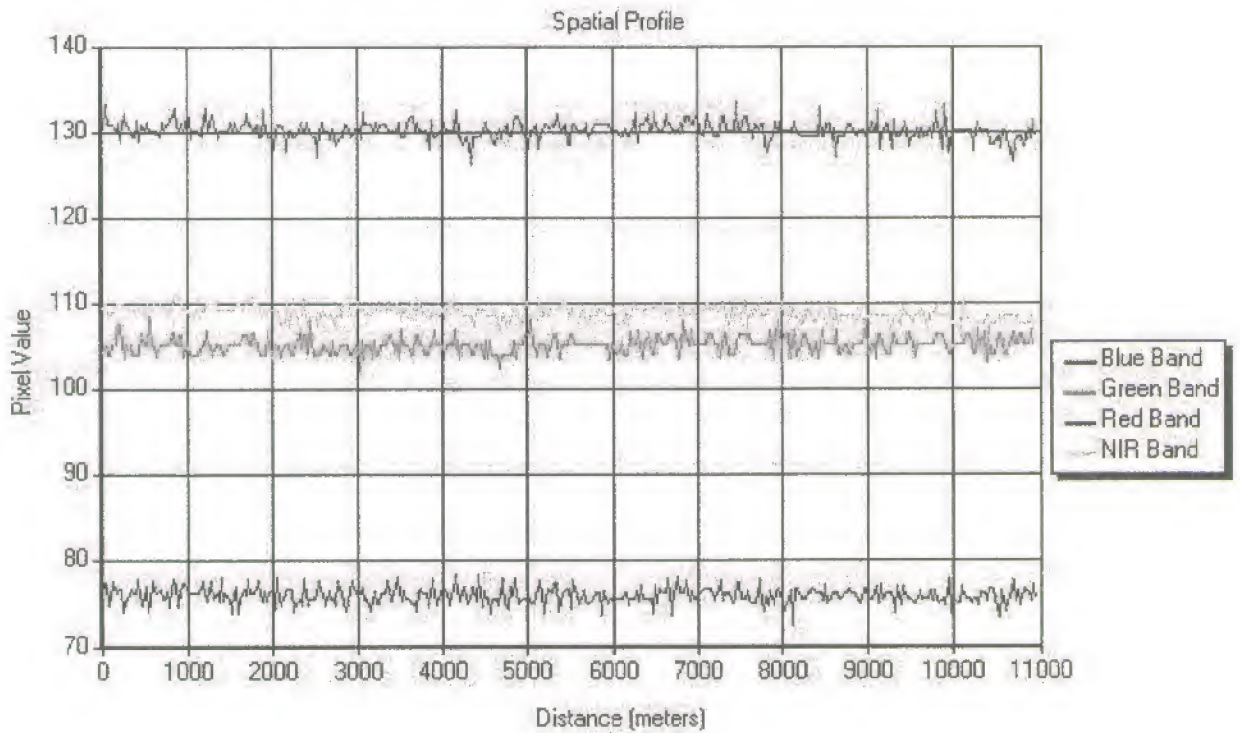


Figure 6. Cross-sectional plot of the ~ 11-km x 1-km area "Libya 1" shown in Figure 5.



Figure 7. A temporal comparison of 11-km x 11-km subsets of a Landsat TM collected on January 7, 1986 (left), an IKONOS image collected on November 3, 2000 (center), and a L7 ETM+ image collected on March 13, 2001 (right) over an area of Mali. RGB: Red, Green, Blue.

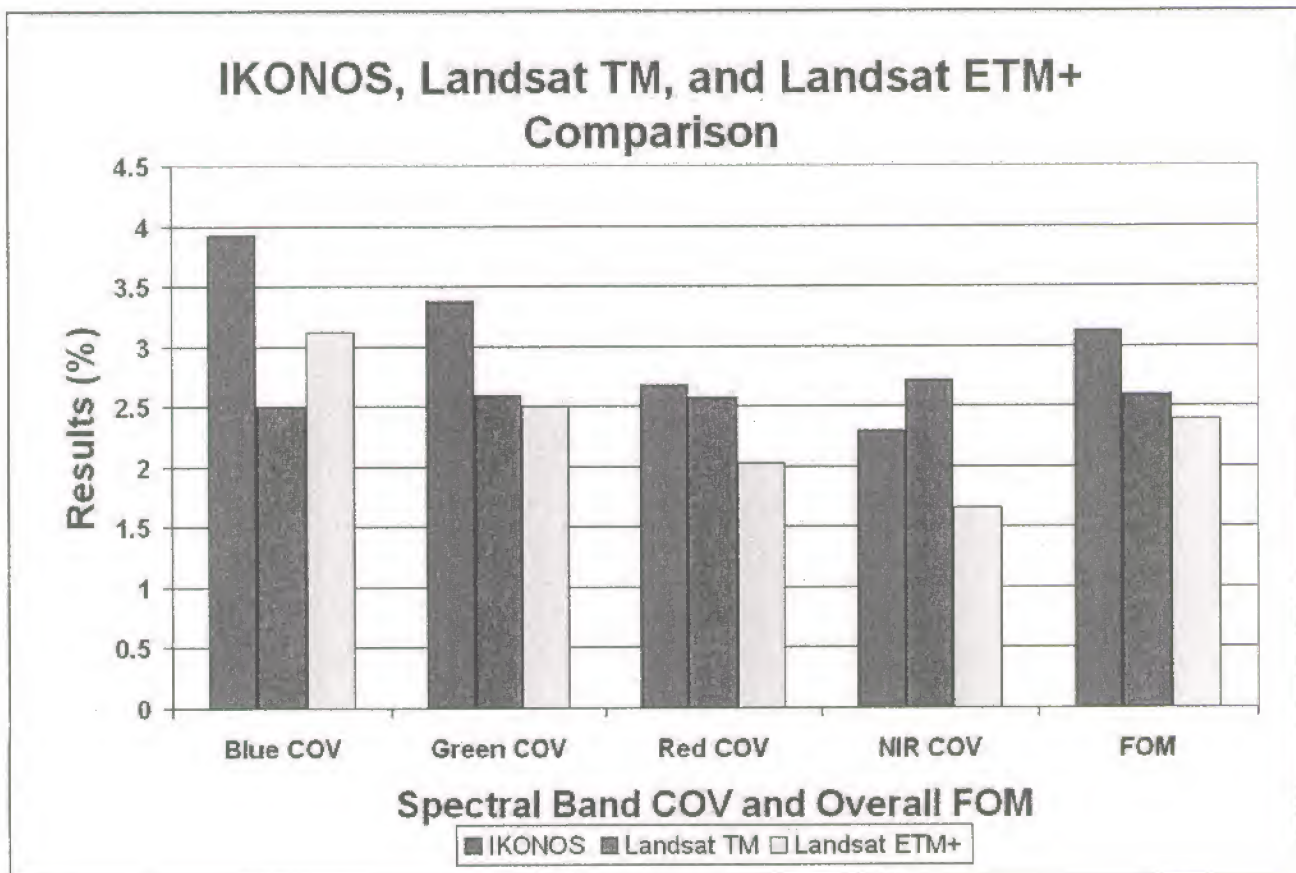


Figure 8. A graph comparing the COVs and FOMs derived from the 11-km x 11-km IKONOS, Landsat TM, and L7 ETM+ images subsets acquired over Mali.

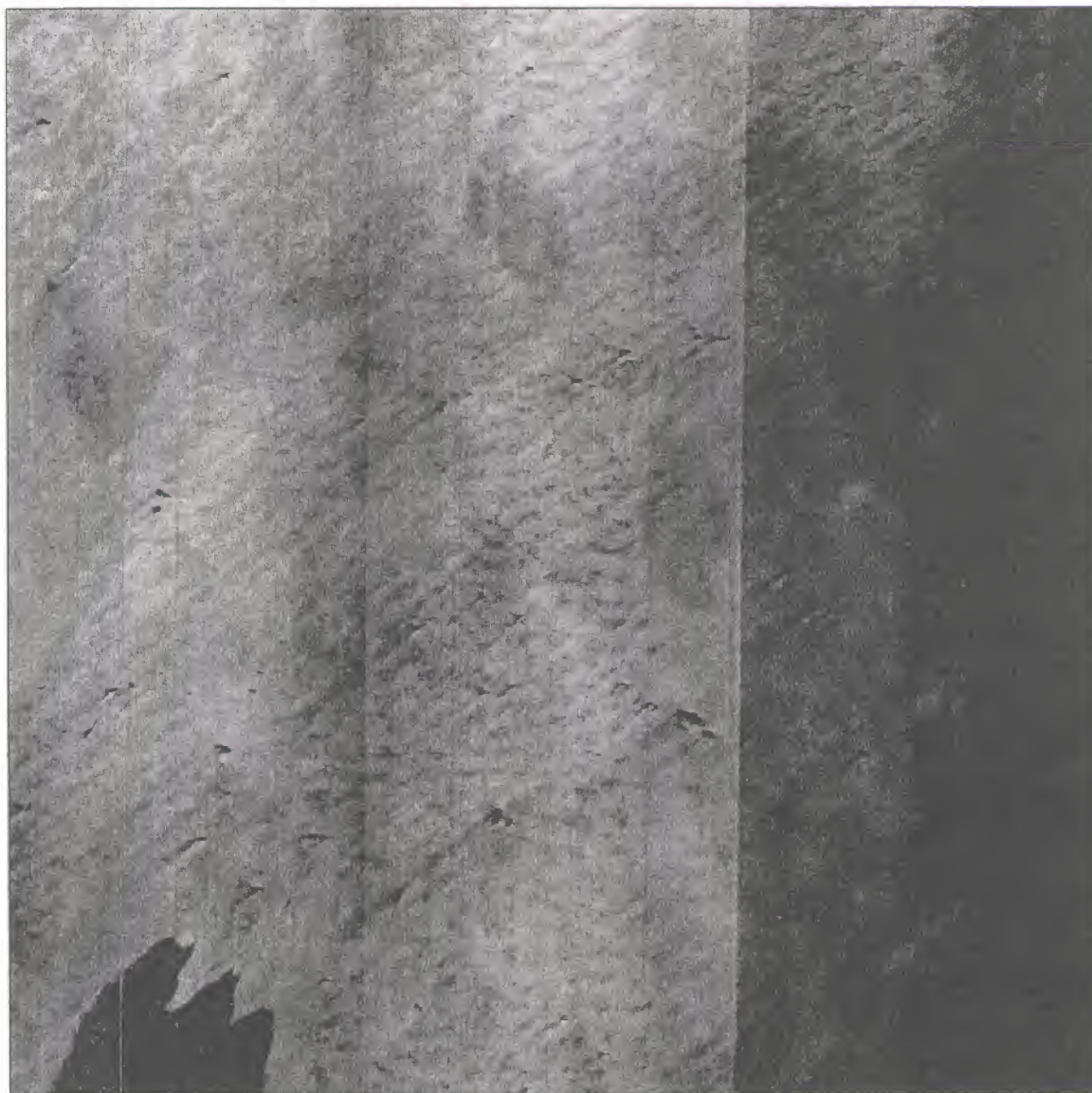


Figure 9. The IKONOS image centered over the ~11-km x 1-km area exhibiting the lowest FOM in the Landsat TM analysis. RGB: 3,2,1.

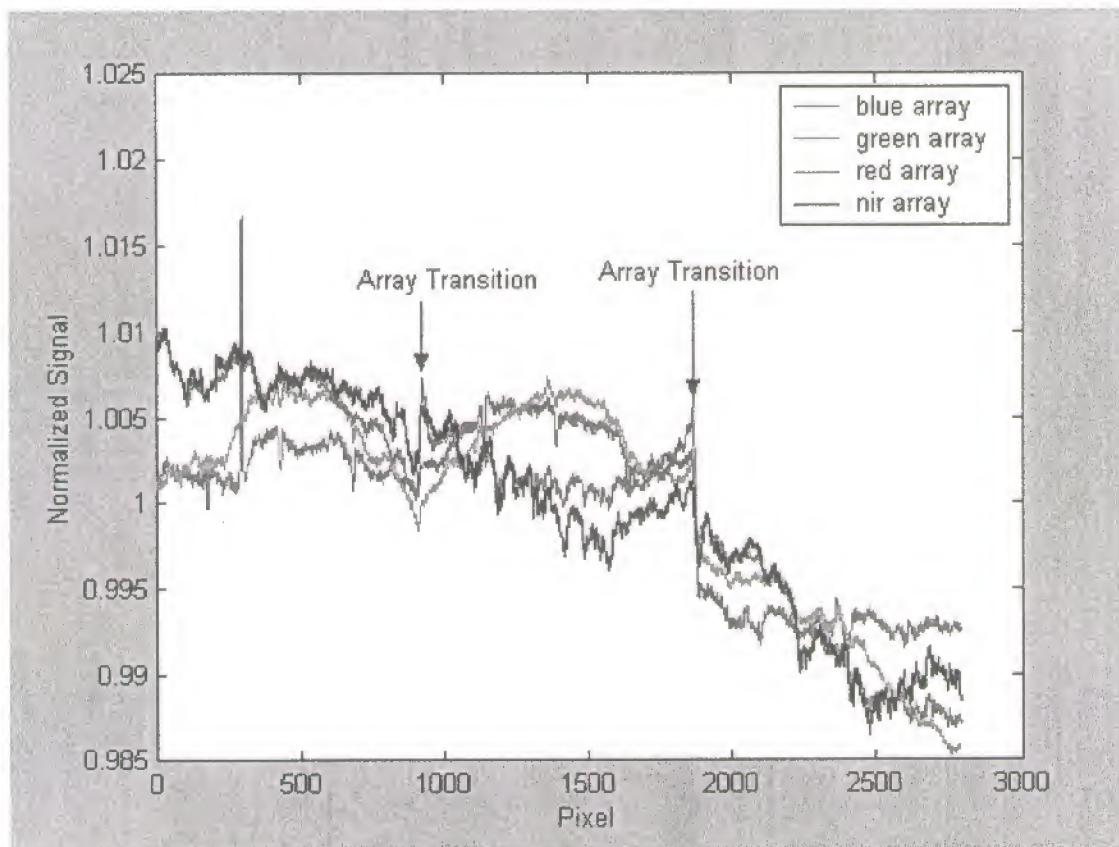


Figure 10. Cross-sectional plot of in-track averaging over the IKONOS Libyan scene showing array differences.

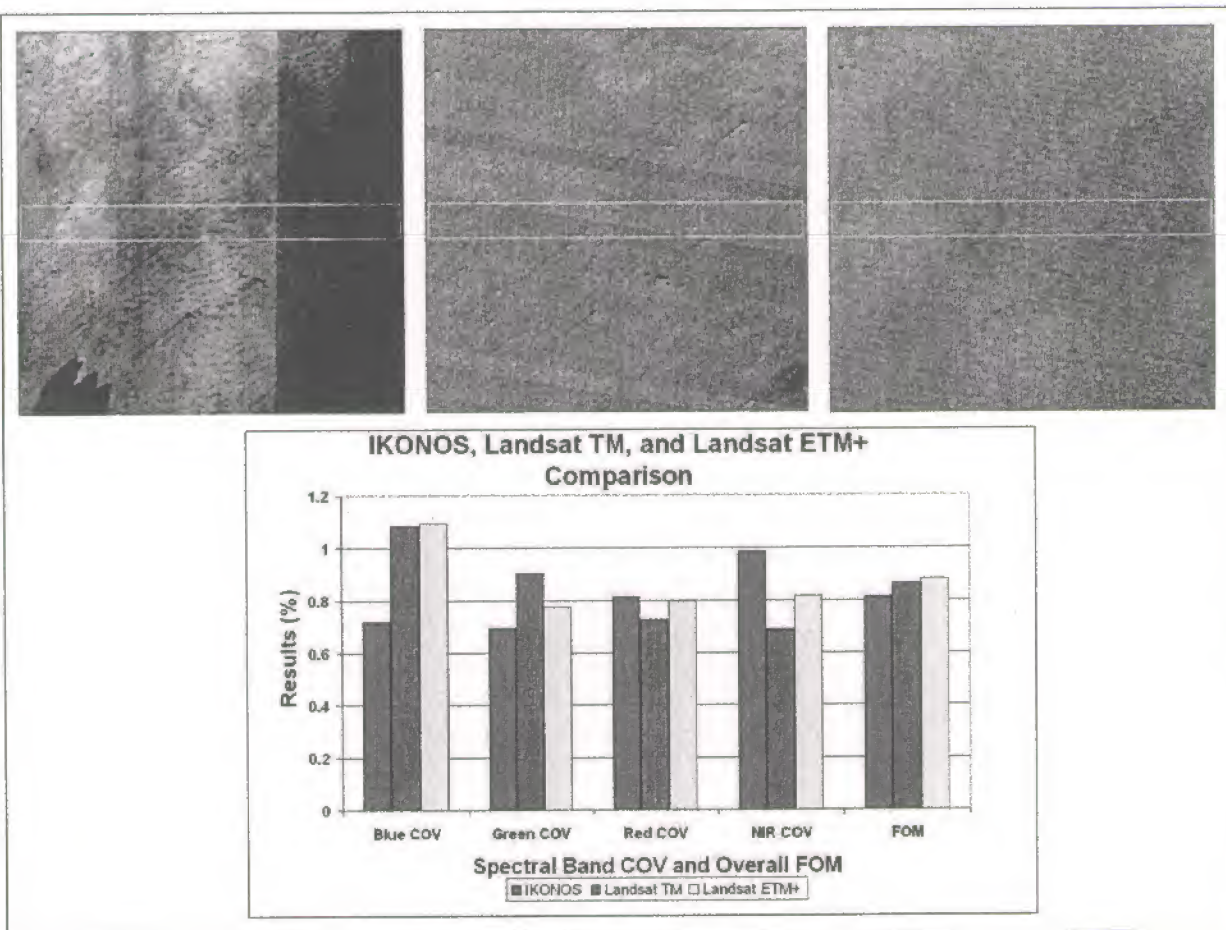
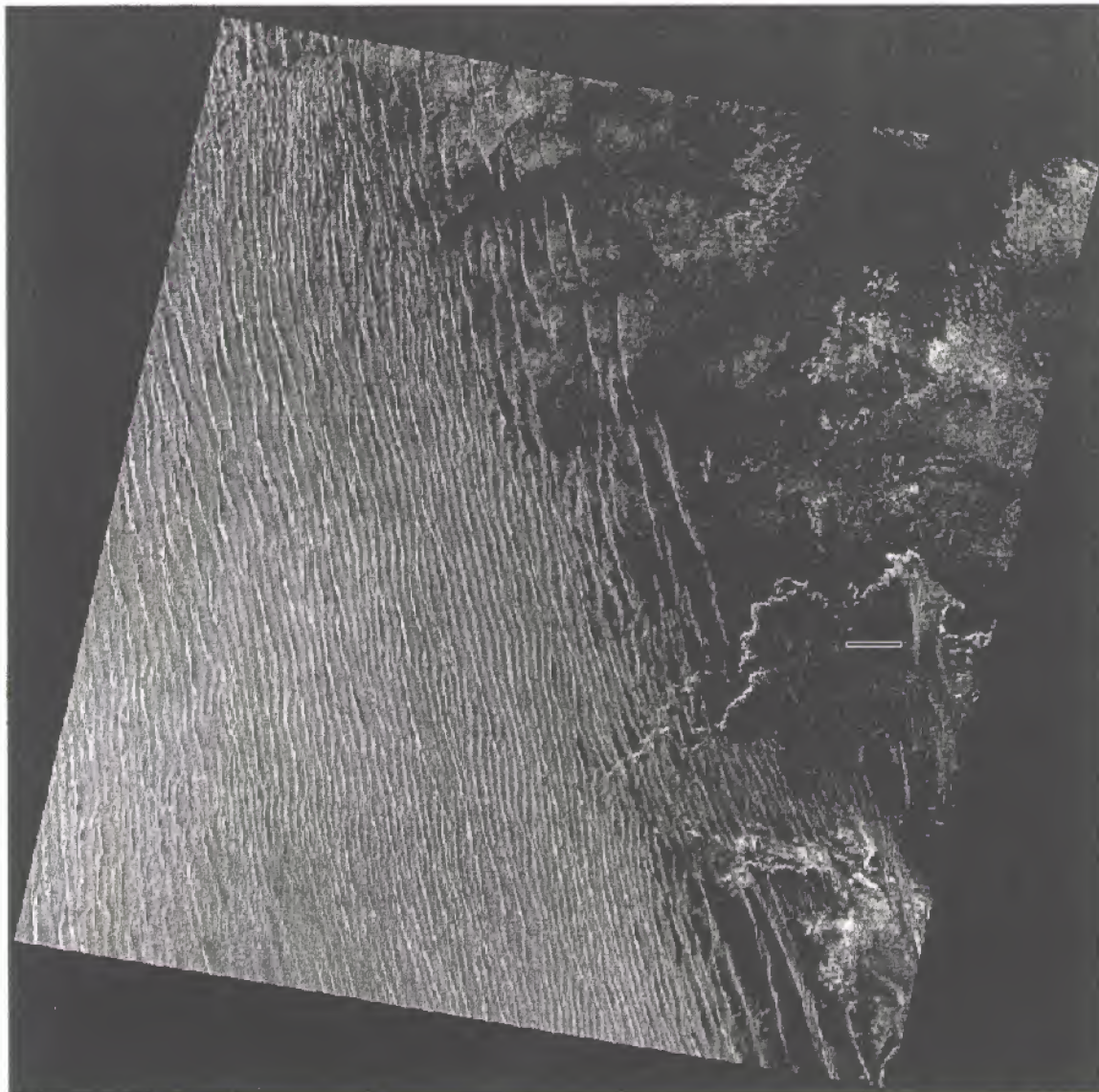
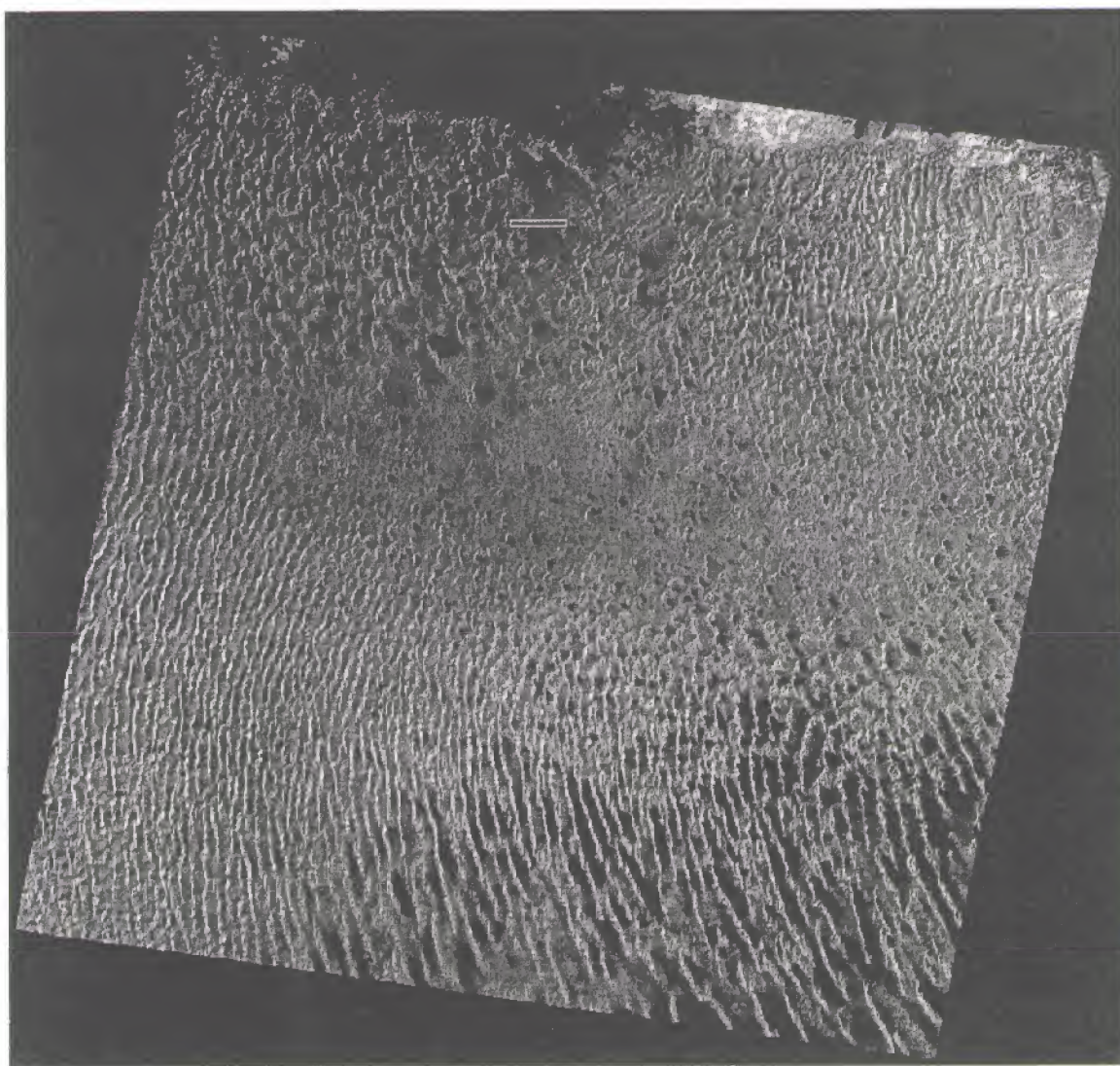


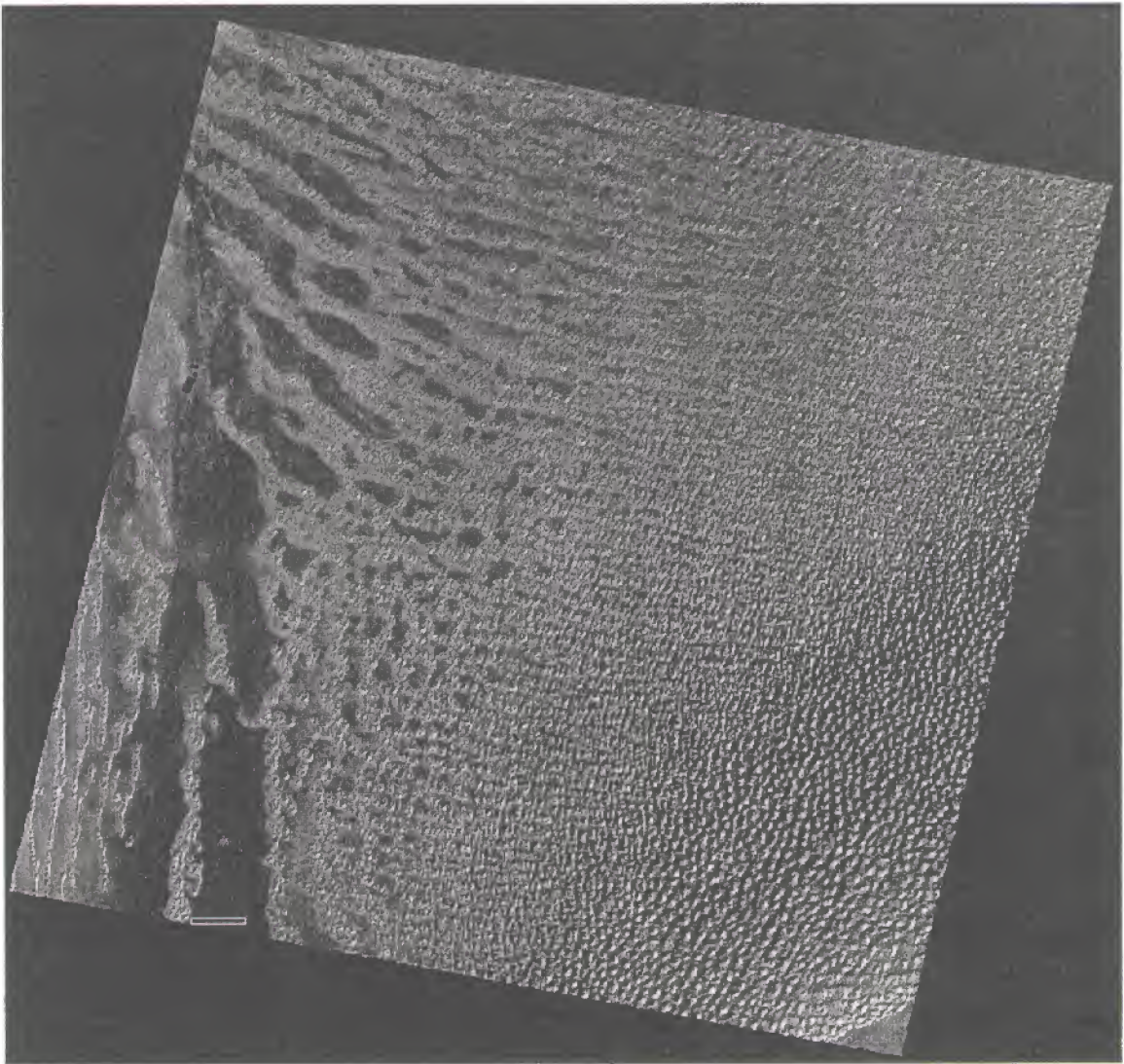
Figure 11. A visual comparison of IKONOS (left), Landsat TM (center), and L7 ETM+ (right) ~11-km x 11-km images over the same location in Libya. We used the ~11- km x 1-km areas contained in the yellow boxes in the COV and FOM calculations presented in the COV and FOM comparison graph below the imagery. RGB: Red, Green Blue.

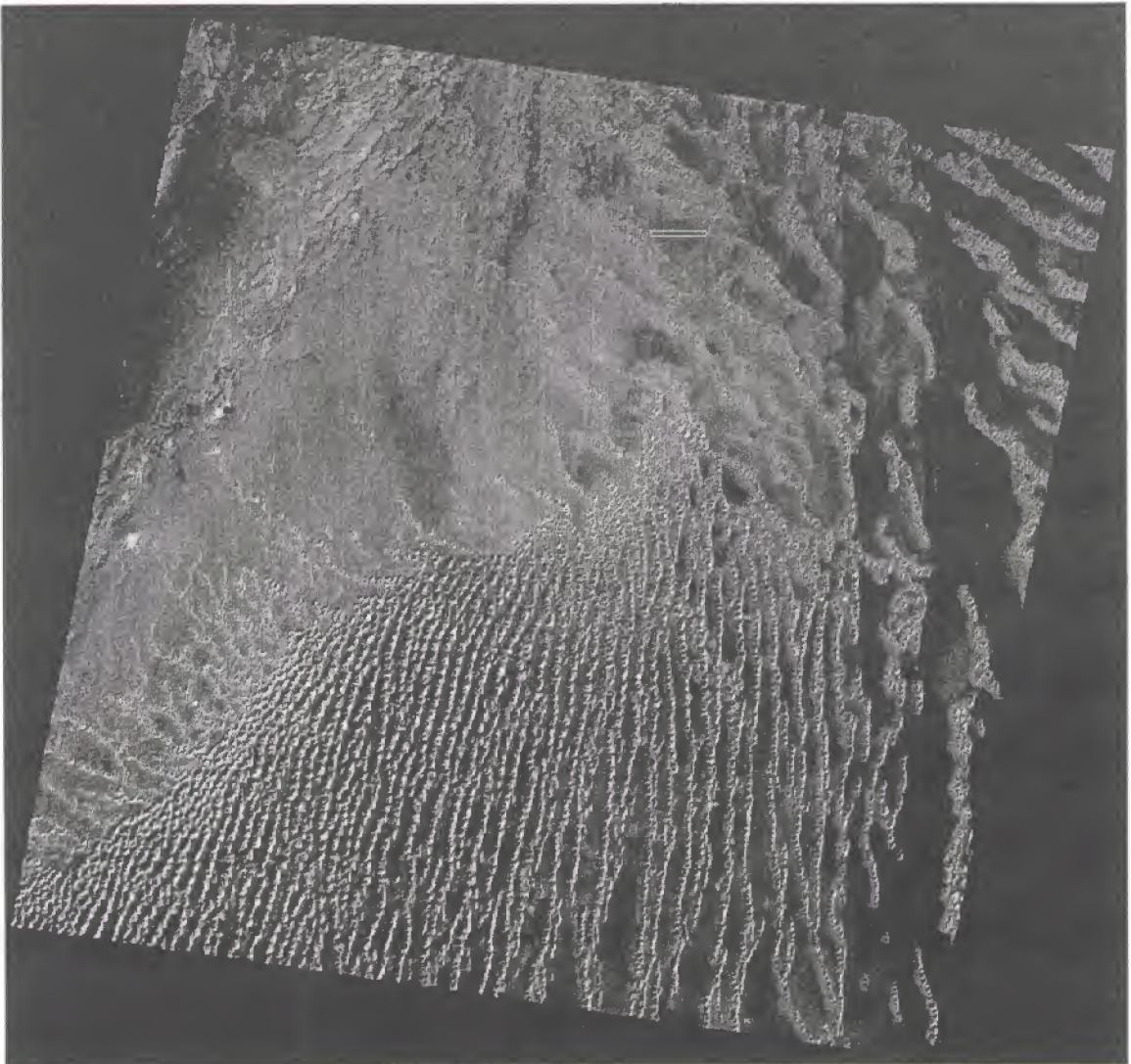
Image Gallery

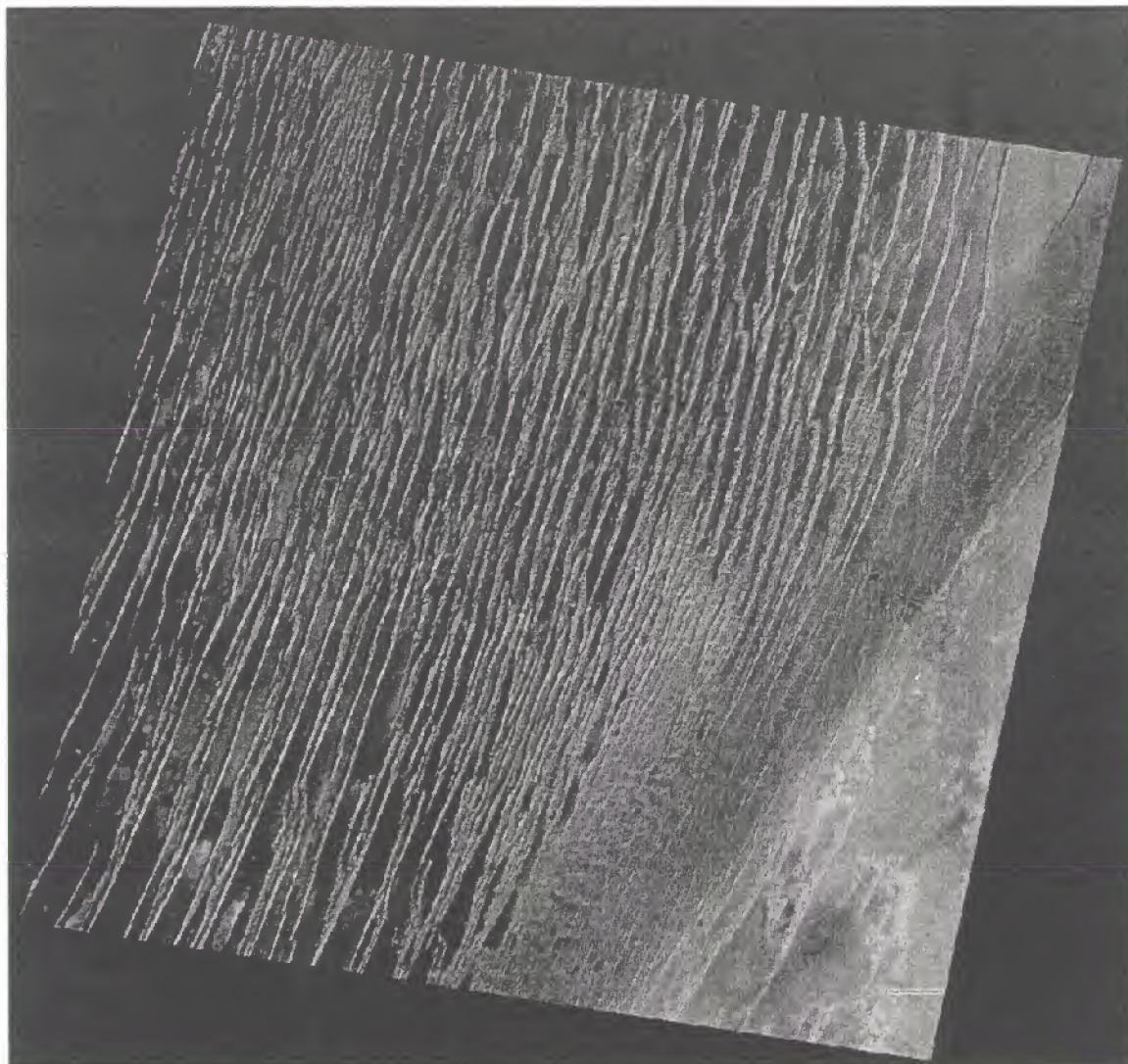
Path 179 / Row 41, Landsat 5, October 20, 1987

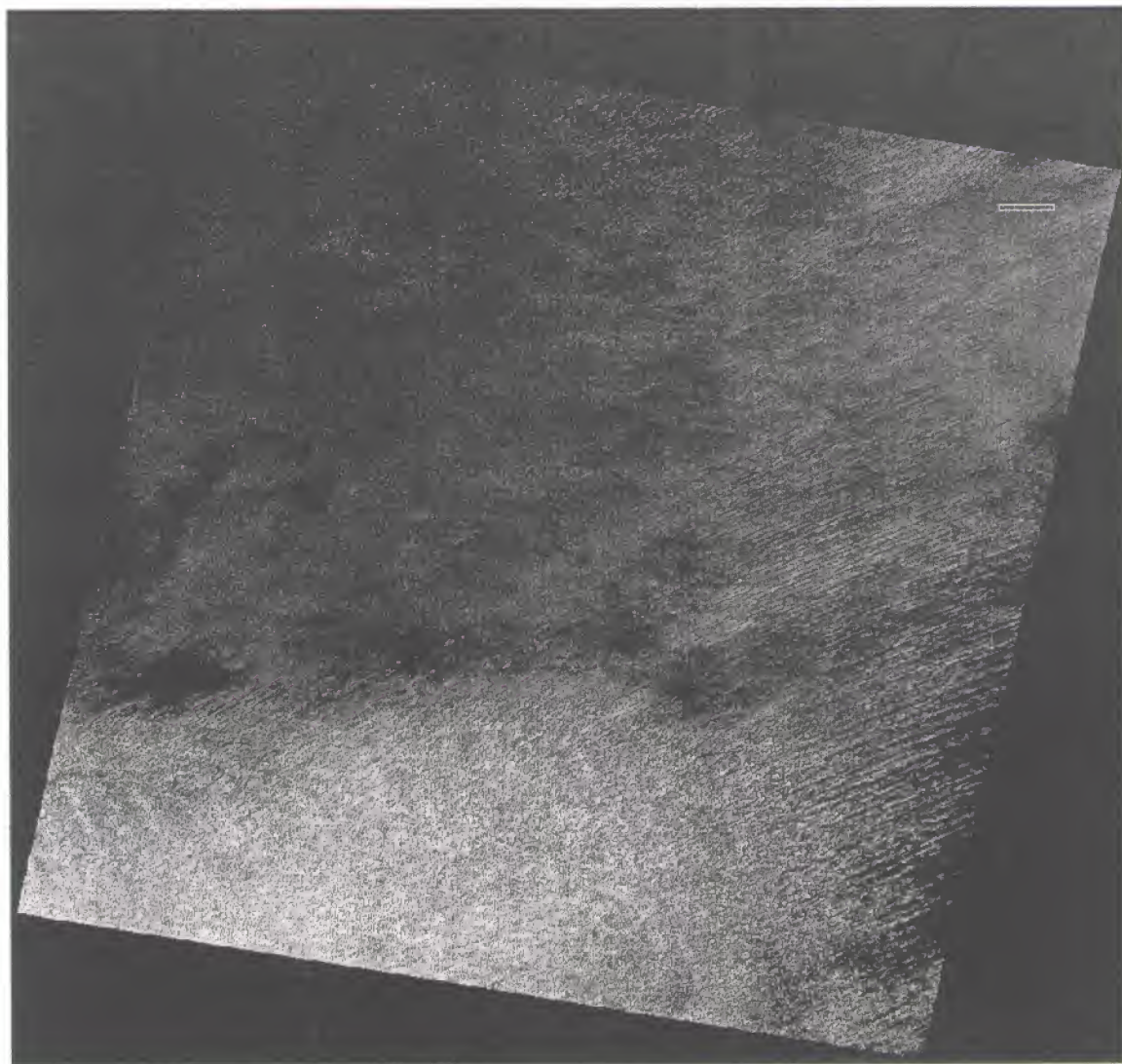


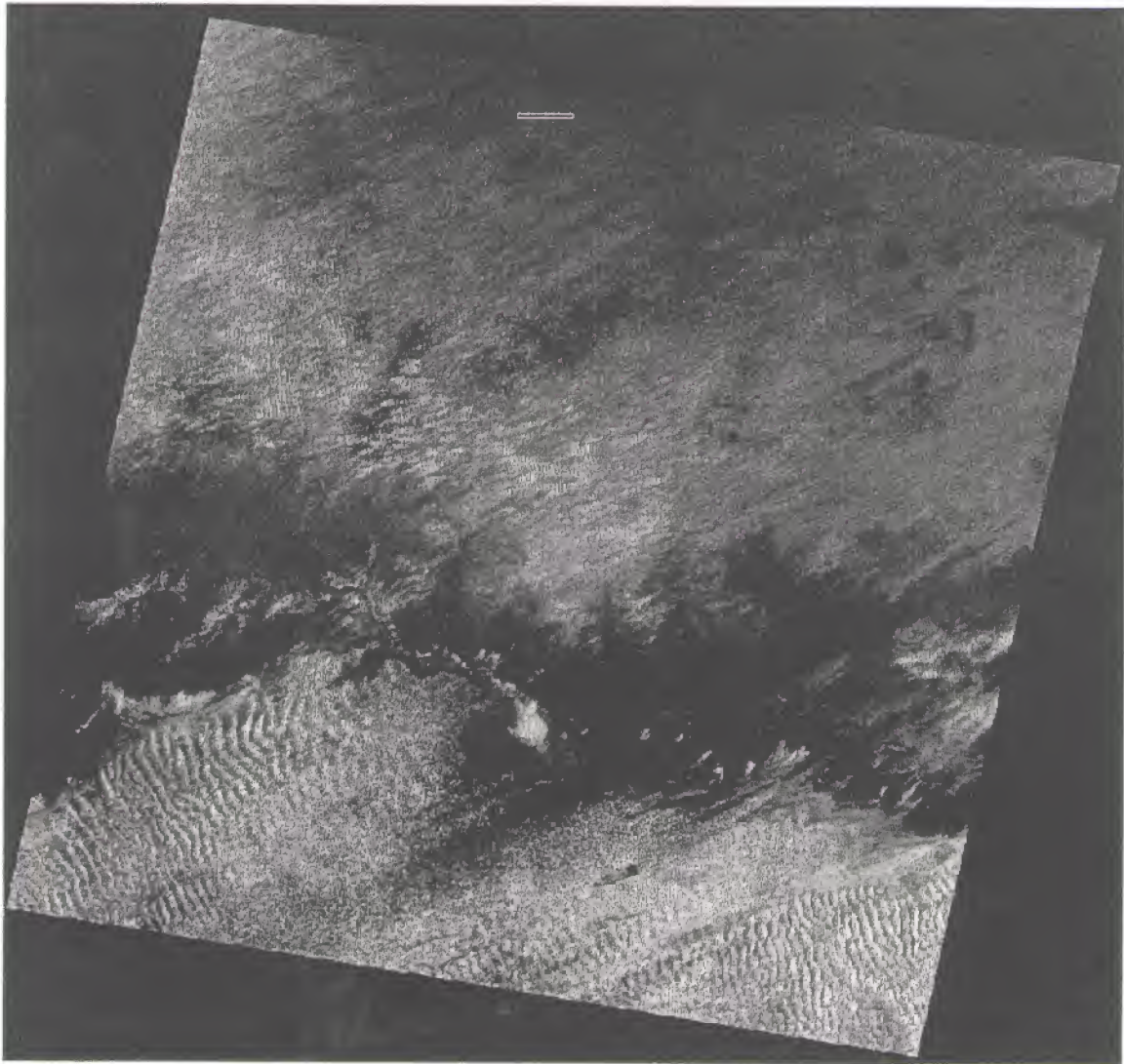












REPORT DOCUMENTATION PAGE					Form Approved OMB No. 0704-0188	
<p>The public reporting burden for this collection of information is estimated to average 1 hour per response, including the time for reviewing instructions, searching existing data sources, gathering and maintaining the data needed, and completing and reviewing the collection of information. Send comments regarding this burden estimate or any other aspect of this collection of information, including suggestions for reducing this burden, to Department of Defense, Washington Headquarters Services, Directorate for Information Operations and Reports (0704-0188), 1215 Jefferson Davis Highway, Suite 1204, Arlington, VA 22202-4302. Respondents should be aware that notwithstanding any other provision of law, no person shall be subject to any penalty for failing to comply with a collection of information if it does not display a currently valid OMB control number.</p> <p>PLEASE DO NOT RETURN YOUR FORM TO THE ABOVE ADDRESS.</p>						
1. REPORT DATE (DD-MM-YYYY) 19-06-2002		2. REPORT TYPE		3. DATES COVERED (From - To)		
4. TITLE AND SUBTITLE Detecting Uniform Areas for Vicarious Calibration Using Landsat TM Imager: A Study using the Arabian and Saharan Deserts				5a. CONTRACT NUMBER NAS13-650		
				5b. GRANT NUMBER		
				5c. PROGRAM ELEMENT NUMBER		
6. AUTHOR(S) Kent Hilbert Mary Pagnutti Robert Ryan Vicki Zanoni				5d. PROJECT NUMBER		
				5e. TASK NUMBER		
				5f. WORK UNIT NUMBER		
7. PERFORMING ORGANIZATION NAME(S) AND ADDRESS(ES) Lockheed Martin Space Operations				8. PERFORMING ORGANIZATION REPORT NUMBER SE-2002-06-00052-SSC		
9. SPONSORING/MONITORING AGENCY NAME(S) AND ADDRESS(ES) Earth Science Applications Directorate				10. SPONSORING/MONITOR'S ACRONYM(S)		
				11. SPONSORING/MONITORING REPORT NUMBER		
12. DISTRIBUTION/AVAILABILITY STATEMENT Publicly Available STI per form 1676						
13. SUPPLEMENTARY NOTES Conference- Refereed paper for Remote Sensing of Environment						
14. ABSTRACT						
15. SUBJECT TERMS						
16. SECURITY CLASSIFICATION OF:			17. LIMITATION OF ABSTRACT	18. NUMBER OF PAGES	19a. NAME OF RESPONSIBLE PERSON	
a. REPORT	b. ABSTRACT	c. THIS PAGE			Mary Pagnutti	
U	U	U	UU	38	19b. TELEPHONE NUMBER (Include area code) (228) 688-2135	